Pramana – J. Phys. (2023) 97:135
https://doi.org/10.1007/s12043-023-02612-2

Theoretical investigation of an array of Josephson junction neuron circuits actuating a mechanical leg and the array in mimicking a multi-legged locomotion

ISIDORE KOMOFOR NGONGIAH[1,*], GAYATHRI VIVEKANANDAN[2], GAETAN FAUTSO KUIATE[3,4], FLORETTE CORINNE FOBASSO MBOGNOU[5] and KARTHIKEYAN RAJAGOPAL[6,7]

[1]Department of Physics, Faculty of Science, University of Bamenda, P.O. Box 39 Bamenda, Cameroon
[2]Centre for Artificial Intelligence, Chennai Institute of Technology, Chennai 600 069, India
[3]Department of Physics, Higher Teacher Training College, University of Bamenda, P.O. Box 39 Bamenda, Cameroon
[4]Department of Mechanical and Industrial Engineering, National Higher Polytechnic Institute, University of Bamenda, P.O. Box 39 Bamenda, Cameroon
[5]Research Unit of Condensed Matter of Electronics and Signal Processing, Department of Physics, Faculty of Sciences, University of Dschang, P.O. Box 67 Dschang, Cameroon
[6]Centre for Nonlinear Systems, Chennai Institute of Technology, Chennai 600 069, India
[7]Department of Electronics and Communications Engineering, University Centre for Research and Development Chandigarh University, Mohali 140 413, India
*Corresponding author. E-mail: ngongiahisidore@gmail.com

MS received 7 November 2022; revised 7 April 2023; accepted 12 April 2023

Abstract. This study aims at the analytical and numerical investigations of Josephson junction (JJ) neuron circuits actuating a mechanical arm and the array. The rate equations for the proposed electromechanical system are established. Numerical simulations of the electromechanical system resulted in a well-defined action potential (AP) and subsequently the actuation of the leg attached to the mechanical arm in an excitable state. Furthermore, the impact of the magnetic field and the effect of mass are as follows: an increase in the magnetic field accelerates the motion of the legs and the amplitude of the displacement decreases with an increase in the mass, and the displacement takes the form of a constant wave for some particular masses as underlined by numerical simulations. A bio-inspired electromechanical system for the locomotion of millipedes and centipedes is proposed and the model failed to propagate the signal in an array of legs since each JJ neuron circuit produces its signal at the same time, because the stimulation is not well-defined by this model of the JJ neuron circuit, despite the advantages of the JJ neuron circuits.

Keywords. Josephson junction neuron circuit; bio-inspired model; electromechanical device; action potential; propagation.

PACS Nos 74.50.+r; 74.81.Fa; 77.65.−j

1. Introduction

Material sciences, superconductivity and nonlinear dynamics have gained research interest with a great focus on the Josephson junction (JJ) which is a theoretical and applied device [1–7]. The possibility of a system emitting high-frequency signals in the ranges of gigahertz and terahertz has been observed in the JJ circuit as opposed to other traditional circuits [8,9]. These systems have practical applications in different areas of research and applied devices including digital logic circuits, voltage standards, detectors, metrology and superconducting quantum interference devices (SQUIDs) just to highlight a few [10–12]. Coupling of arrays of JJ has solved the difficulties of low output by single JJ circuits as highlighted by various studies [8,9,13–16]. The vast variation of frequencies exhibited by the JJ circuits can be used in actuation mechanisms at both micro and macrolevels, which can result in high-frequency electromechanical systems (when the JJ is coupled to a mechanical system) [17,18]. Researchers and engineers are concerned with the design of a large

Published online: 29 August 2023

ensemble of electromechanical actuators in mimicking the locomotion of multi-leg organisms like centipedes and millipedes. Such characteristics can be observed by coupling the electromechanical devices via their mechanical or electrical dimensions in which synchronisation can be obtained [19]. Similar to the growth of the computer and internet some years back, robots are gaining ground in many applications. This is in close collaboration with the ways humans interact with artificial intelligence and machines, which is much similar to the biological systems. Robotics is applicable in different fields and aspect of real life: Healthcare robotics (for medical delivery, evaluation, monitoring and helping health care practitioners in specific tasks) [20,21], medical and surgery robotics (for exactness and minimum invasive routine) [22], body–machine interfaces (for amputees assistance) [23], telepresence robotics [24], cyborgs, exoskeletons and wearable robotics [25], humanoid robotics [26], industrial robotics (for industrial automation activities, gripper) [27], housekeeping (robot cleaners) [28], collaborative robots (domotics and public spaces automation coordinators) [29], military robotics (navigators and drones) [30], underwater, flying and self-driving machines (self-piloting) [30], space robots (space missions) [31], entertainment (games, toys) [32], art robotics (creative robotics for beauty) [33], environmental and alternately powered robots [34], swarm and microbots (for environmental emergency exploration) [35], robotic networks (for accessing and sharing of information and database) and lastly modular robotics [36]. Advancing these technologies to a greater extent, an interesting research era must be observed for satisfactory applications highlighting accuracy, cost effectiveness, reliability and speed [37]. These robots perform tasks which are hazardous to humans including defusing bombs and mines and exploring shipwrecks. Recently, robots are also inspired by nature, giving way to the domain of bio-inspired robotics. Bio-inspired robotics is concerned with the study of biological systems and their mechanisms for practical applications in engineering. These applications include bio-sensors (similar to the eye), bio-actuators (such as the muscle) and bio-materials (such as the spider silk). These systems are characterised by the type of the locomotion system [38]. Research activities in this regard have sought to unveil the mechanism of walking applied to practical robotics [39–41]. In this, the major challenges to be considered are firstly to control an exorbitant number of elements and how to investigate the locomotion for a particular task [42,43]. In the literature, the dynamics of an array of identical cells have been investigated which have been compared with the phase relationship in the gaits of legged animals [44–50] and other living organisms such as the lamprey [51–54] with movement pattern associated with travelling waves of muscle contractions. The word 'cell' is elaborated mathematically by a system of differential equations. Irrespective of physiological considerations, central pattern generators (generation of animal locomotion) like arrays of cells (similar to the electronic schematics) capture great interest in the design, modelling and control of legged locomotion due to the variation in phase relationships stably and naturally [55,56]. Kopell and Ermentrout [57–59] showed that a linear array made up of several coupled similar cells can exhibit travelling wave motions similar to those recorded in the locomotion of lamprey and other biological observations made by these models have been reported in [53,60]. Considering the living organisms with fewer legs, the finding of Collins and Stewart [45] paved the way for the observation of a natural pattern of oscillation in an identical array of coupled cells, similar to those recorded in gaits, such as the quadrupeds, bipeds and hexapods which are characterised by similar phase relationships. Motivated by the above literature, we envisage using the advantages of JJ such as the generation of electrical energy (generation of voltage); production of stereotypical voltage spikes comparably to the action potential (AP) in neurons in response to stimulation current; firing thresholds and refractory periods [61] to propose another approach to simulate the motion of myriapods by using an array of JJ neuron circuit coupled to a mechanical arm. Coupling two JJs to a JJ neuron circuit as demonstrated in this work is advantageous in that, the respective junctions behave typically the same as ion channels in which the depolarising current (like Na^+) and the hyperpolarising current (like K^+) represent both junctions [61,62]. The model exhibits interesting characteristics of natural biological neurons especially the evocation of an AP (firing) as a consequence of the excitation currents or pulses, input strength limit (thresholds) below which no AP is produced and refractory duration taken after firing for which another AP is not feasible [62,63]. Furthermore, another aspect of using this junction overcomes the ancient scaling difficulties encountered in computational neuroscience [64–66]. The characteristic of being easy to manufacture since a great number could be incorporated on a chip and fairly inexpensive is giving the junction an interesting aspect of research. The ability of the junction to be faster than computer simulations of neurons or real biological neurons is observed daily, especially in the light of a Josephson neuron AP lasting for a picosecond, which is approximately a billion times shorter than a biological AP [61].

The paper is arranged as follows: Section 2 discusses the array of JJ neuron circuits actuating a mechanical leg, §3 considers several lines of JJ neurons coupled in

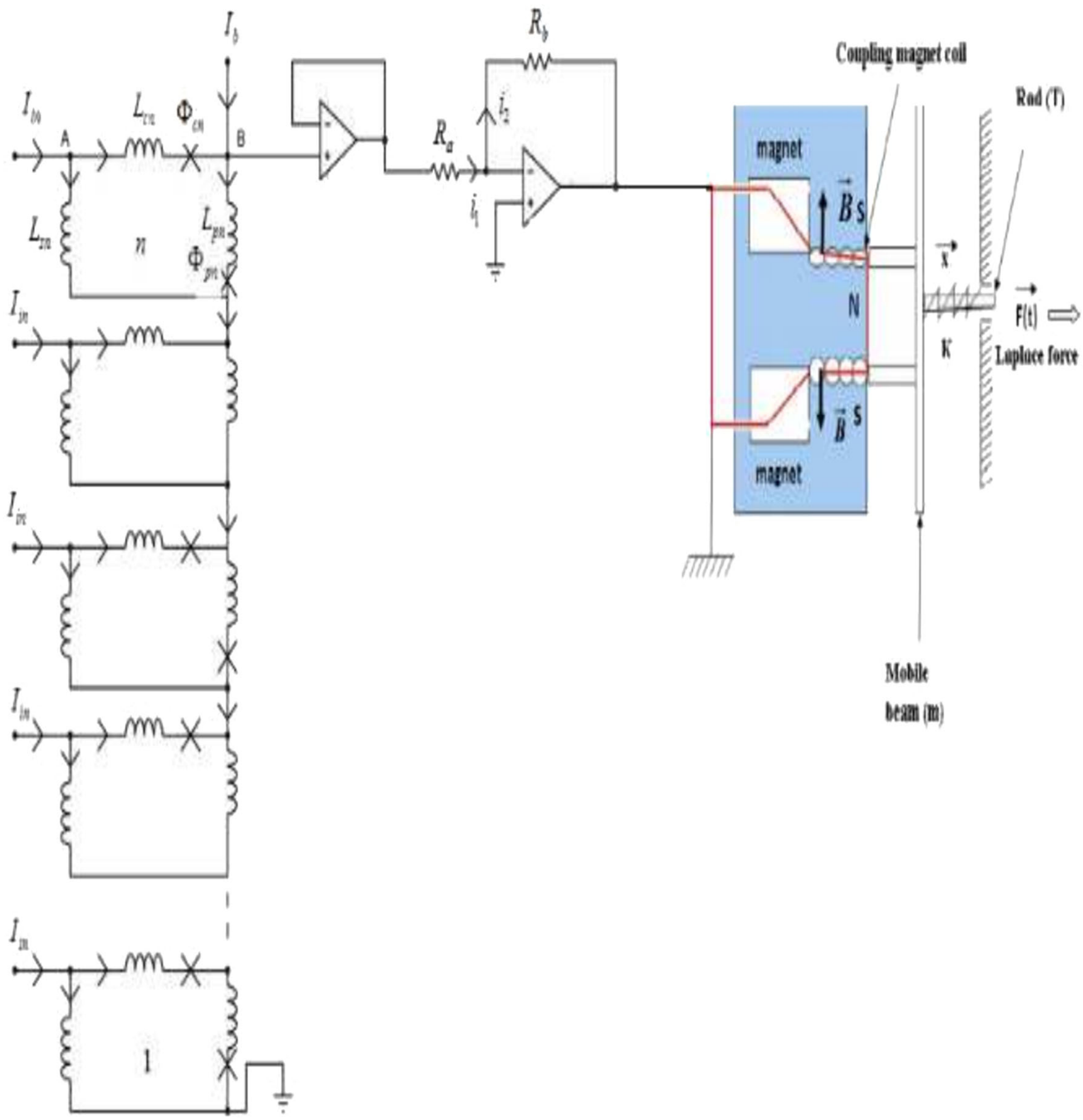

Figure 1. Schematic of the electromechanical system.

actuating an array of mechanical legs and finally, the conclusion is presented in §4.

2. Array of JJ neuron circuits actuating a mechanical leg

The electromechanical system shown in figure 1 reports the propagation of electrical signals and the walking motion of one leg.

Figure 1 is an electromechanical system consisting of electrical and mechanical parts. The electrical part is an array of N-coupled JJ neuron circuits, in which a single JJ neuron circuit couples two JJ in a superconducting loop referred to as the pulse junction (p) and control junction (c) with two stimulation currents normalised to I_{op} refer to as the input current I_{in} and the excitation current I_b. The mechanical part is made up of a movable mobile beam of mass m that is attached to the leg T with similar motion and has an instantaneous displacement x. Two ideal amplifiers are introduced to couple the electrical part to the mechanical part, so as to minimise any perturbation during the propagation of the AP and are modelled as

$$\sum_{n=1}^{N} V_n' = -\frac{R_b}{R_a} \sum_{n=1}^{N} V_n, \tag{1}$$

where V_n' is the output voltage of the second operational amplifier and V_n is the total voltage of the interconnected neurons. The first ideal amplifier is supposed to maintain the same voltage coming from the electrical part and the second amplifier is for amplification (this simplifies the coupling between the electrical and mechanical parts since the human body is associated with continuous regeneration of neurons). For the external excitation of the electrical part, some recurrence relation for I_b is defined as

$$I_{an} = I_b + (N - n)I_{in}, \tag{2}$$

where I_{an} is the bias current of each neuron and I_{in} is its input current. To simplify the highlighted model, the following relation is considered:

$$(I_{in})_n = (I_{in})_{(n-1)} = (I_{in})_{(n-2)} = \cdots = (I_{in})_2. \tag{3}$$

The circuit parameters are the indicated branch inductances L_s, L_p and L_c which are scaled by adding them up to L_{Total} which is reduced to Λ_s, Λ_p and Λ_c. Applying Kirchhoff's and Newton's laws to figure 1, the following dimensionless differential equations are obtained:

$$\begin{aligned}\frac{\mathrm{d}V_{pn}}{\mathrm{d}\tau} =& -\Gamma V_{pn} - \sin(\Phi_{pn}) - \lambda(\Phi_{pn} + \Phi_{cn})\\ &+ (1 - \Lambda_{pn})i_b\\ &+ [\Lambda_{sn} + (1 - \Lambda_{pn})(N - n)]i_{in},\end{aligned} \tag{4a}$$

$$\begin{aligned}\frac{\mathrm{d}V_{cn}}{\mathrm{d}\tau} =& -\Gamma V_{cn} - \sin(\Phi_{cn}) - \lambda(\Phi_{pn} + \Phi_{cn})\\ &+ [(N - n) + \Lambda_{sn}]i_{in} - \Lambda_{pn}i_b,\end{aligned} \tag{4b}$$

$$\frac{\mathrm{d}\Phi_{pn}}{\mathrm{d}\tau} = V_{pn}, \tag{4c}$$

$$\frac{\mathrm{d}\Phi_{cn}}{\mathrm{d}\tau} = V_{cn}, \tag{4d}$$

$$\begin{aligned}\frac{\mathrm{d}i}{\mathrm{d}\tau} =& \delta y - \sigma i + \rho \sum_{n=1}^{N}\\ &\times \left[\left(\frac{\phi_0}{2\pi} - \lambda\Lambda_p I_{op}\right)V_{pn} - \lambda\Lambda_p I_{op} V_{cn}\right],\end{aligned} \tag{4e}$$

$$\frac{\mathrm{d}y}{\mathrm{d}\tau} = \mu i - \beta y - \gamma x, \tag{4f}$$

$$\frac{\mathrm{d}x}{\mathrm{d}\tau} = y, \tag{4g}$$

where $\lambda = \phi_0/2\pi L_{\text{Total}} I_{op}$ is the coupling parameter, μ is a geometric parameter, Γ is the normalised drag constant, l_p is the inductance of the real mechanical part, r_p is the internal resistance of the coil, k is the spring constant, $\lambda\!\!\!^-$ is the coefficient of friction force, l is the length of the electrical wire inside the magnetic field B, t is the time, with the following dimensionless variables:

$$\begin{aligned}\tau &= \omega_\tau t, \quad \mu = \frac{BlI_{op}}{m\omega_\tau^2 X_0},\\ \beta &= \frac{\lambda\!\!\!^-}{m\omega_\tau}, \quad \gamma = \frac{k}{m\omega_\tau^2},\\ \delta &= \frac{BlX_0}{l_p I_{op}}, \quad \sigma = \frac{r_p}{l_p\omega_\tau},\\ \rho &= \frac{R_b}{l_p I_{op} R_a}, \quad V_p = \dot{\Phi}_p, \quad V_c = \dot{\Phi}_c\end{aligned}$$

with ω_τ the frequency of the system and X_0 a constant. It is worth highlighting that system (4) elaborates on the propagation of electrical signals and the motion of one leg of the myriapods. The two JJ are linked by the inductor to form the JJ neuron circuit as elaborated in the third term of eqs (4a) and (4b) and furthermore, the network is obtained by connecting the JJ neuron circuits in series elaborated by the subscript n in the set of eq. (4). The parameters used in the numerical simulations are taken in [2,4,17,67,68]. The system of equations coordinating the mechanical part is given in eqs (4e)–(4 g). The parameters of the simulation are highlighted in table 1.

Taking a small value of the incoming currents $i_{in} = 0.0001$ and $i_b = 0.0001$, the AP is presented in figure 2.

Figure 2 presents the different AP given by the pulse junction on the model, the control junction on the same model and the net voltage for an array of five neurons ($n = 1, 2, \ldots, 5$). The observation of an AP in which

Table 1. Parameters of the electromechanical system.

Parameters	Values
I_{op}	0.2
Λ_c	0.0
Λ_s	0.5
Λ_p	0.5
λ	0.1
η	1.0
$\lambda\!\!\!^-$	0.001
Γ	1.5
i_{in}	0.21 mA
R	12.7 Ω
R_a	1 Ω
ω	1000
X_0	0.001
B	0.00156 T
l_p	10 mH
R_b	1 Ω
l	300 m
m	12×10^{-7} kg
λ	2.9 kg s^{-1}
k	20 Nm^{-1}

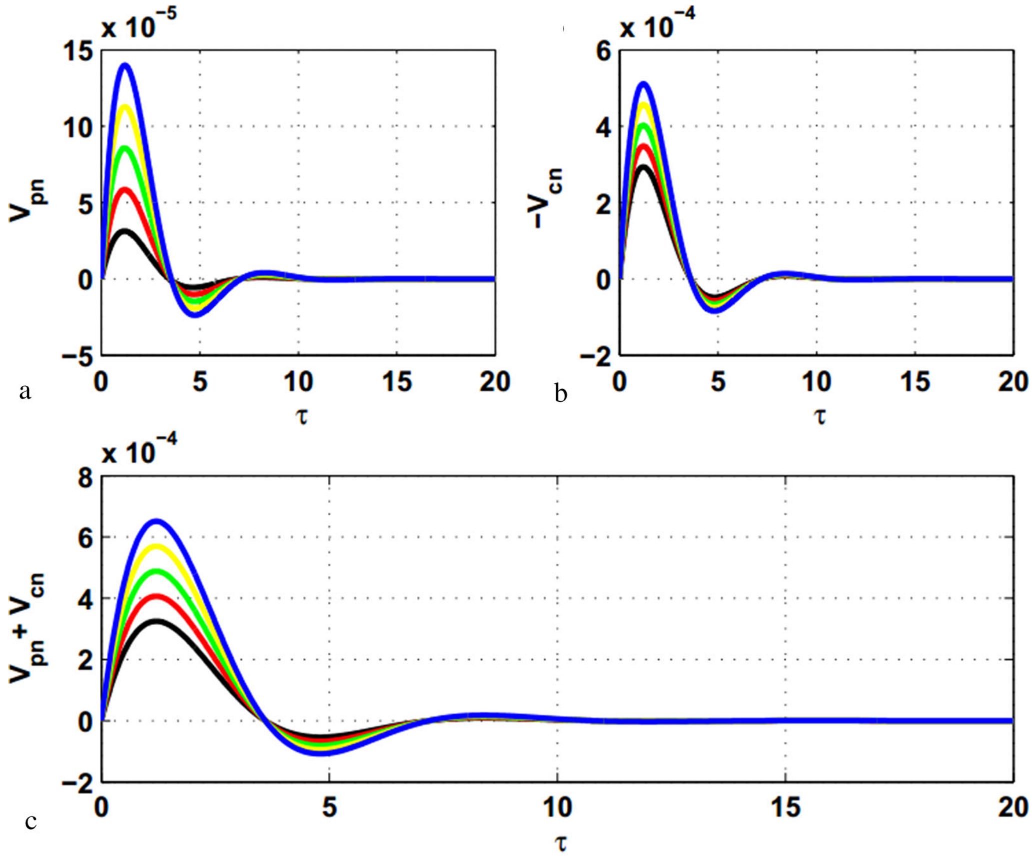

Figure 2. Time evolution of the AP: (**a**) for pulse junction V_{pn}, (**b**) for the control junction V_{cn} and (**c**) net AP $V_{pn} + V_{cn}$. The black curve is for the fifth JJ neuron circuit, the red curve is for the fourth JJ neuron circuit, the green curve is for the third JJ neuron circuit, the yellow curve is for the second JJ neuron circuit and the blue curve is for the first JJ neuron circuit.

the number of AP increases with an increase in the number of JJ neuron circuits interconnected is a consequence of the local stimulation of a whole nerve. The AP of the fifth neuron is the smallest while the others are added by an increase in amplitude. This looks like an effect of the parallel AP created in the system, hence not a desirable response since it does not depict the behaviour of neurons connected where one AP is observed and not the case of figure 2 where the number of AP equals the number of JJ neuron circuits. Such an effect of local stimulation is because of the influence of each input current passing through the neuron and the influence of the bias current. These currents are very important in different JJ elements but cannot be considered exactly as the stimulation in the JJ neuron circuit, the reason for such behaviour. The time evolution of the current feeding the mechanical arm and the instantaneous displacement of the mobile beam are present in figure 3.

From figure 3, the membrane potential is observed to remain lower and consequently the current is very small in intensity (approximately to the order 10^{-4}) to provoke an instantaneous displacement of the mobile beam which has a weak amplitude (10^{-6}). For $0.1 \leq i_b \leq 1$, the system is observed to be in an excitable state. The curves in figures 4 and 5 are presented for the specific value $i_b = 0.8$.

Figure 4 shows that the electromechanical system represented by system (4) can generate a membrane potential with an intensity sufficient enough for actuation processes in the excitable state. In the excitation process, the membrane potential is uniform over the whole membrane. This is an interesting response as it is observed in a natural biological system like the human body, especially when they are an interconnection of neurons. The time series of the current feeding the mechanical system and the instantaneous displacement of the mechanical arm are presented in figure 5.

In the excitable state, there is a uniform AP in the array of neurons (see figure 4) in which the propagation of this nerve impulse generates a current as shown in figure 5a which is significant to provoke an instantaneous displacement of the mobile beam, which in essence is the actuation of the leg as depicted in figure 5b. These results are interesting with scientific impact and it is verified that there is a certain range of values of the

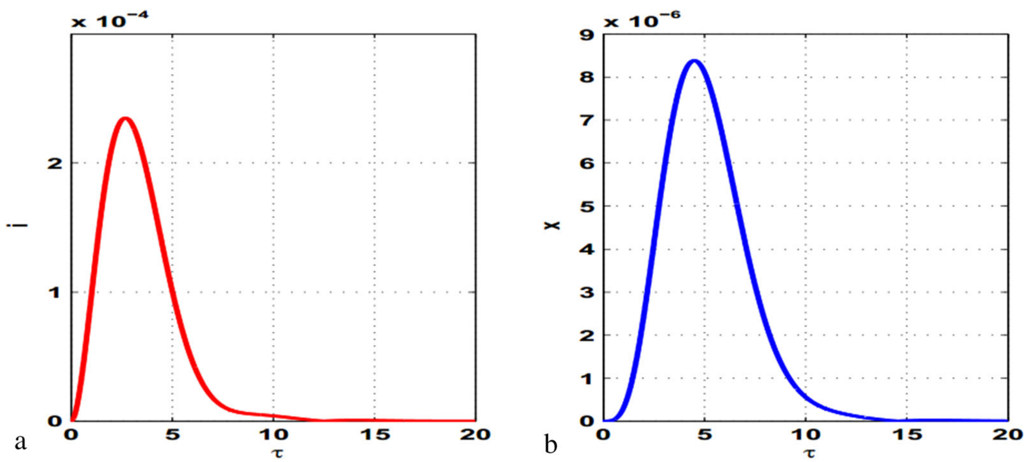

Figure 3. Time evolution of (**a**) current i powering the mechanical device and (**b**) the instantaneous displacement x of the mobile beam.

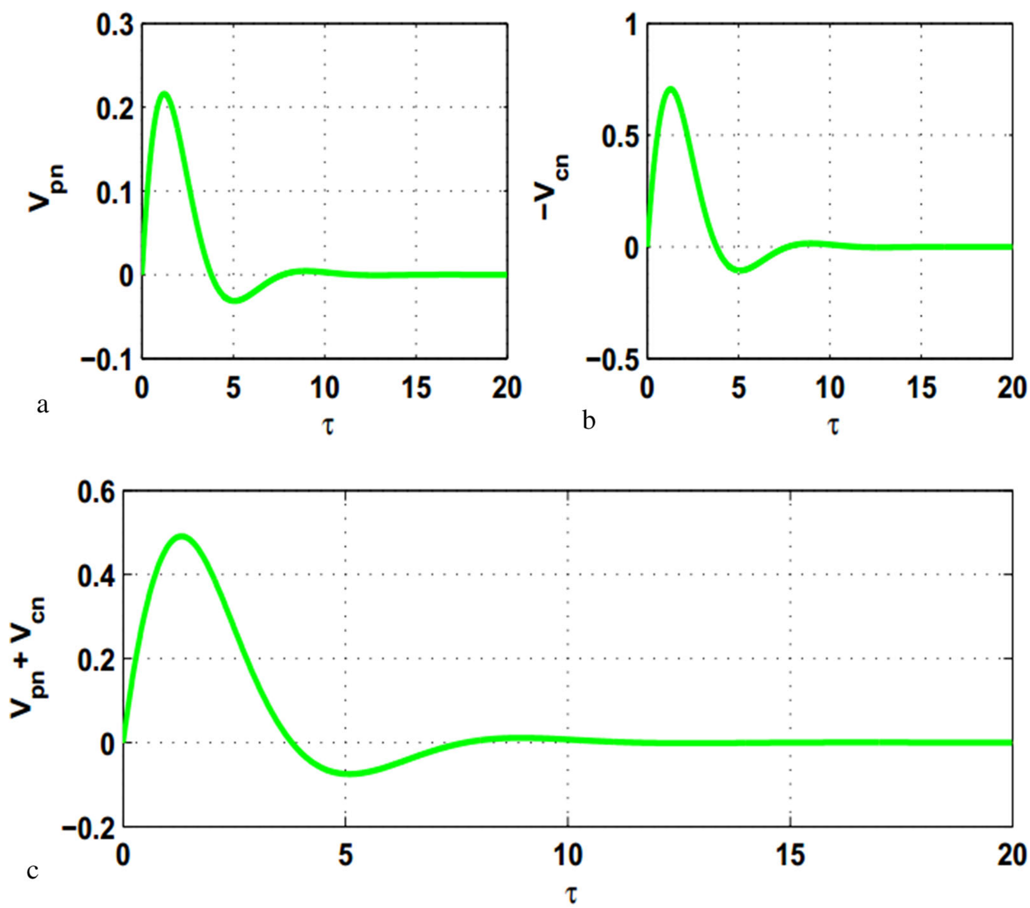

Figure 4. Time evolution of the AP in an excitable state: (**a**) for the pulse junction V_{pn}, (**b**) for the control junction V_{cn} and (**c**) net AP $V_{pn} + V_{cn}$.

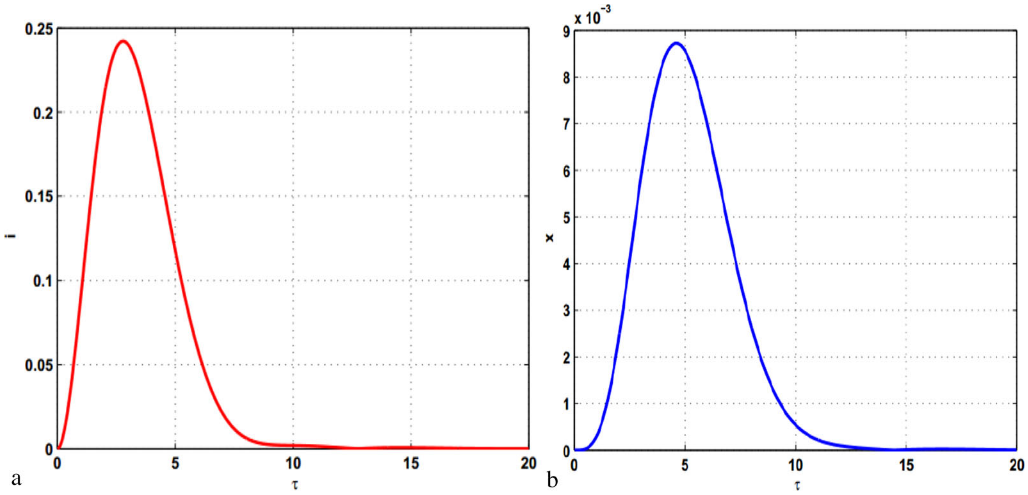

Figure 5. Time evolution in an excitable state of (**a**) current i powering the mechanical device and (**b**) the instantaneous displacement x of the leg.

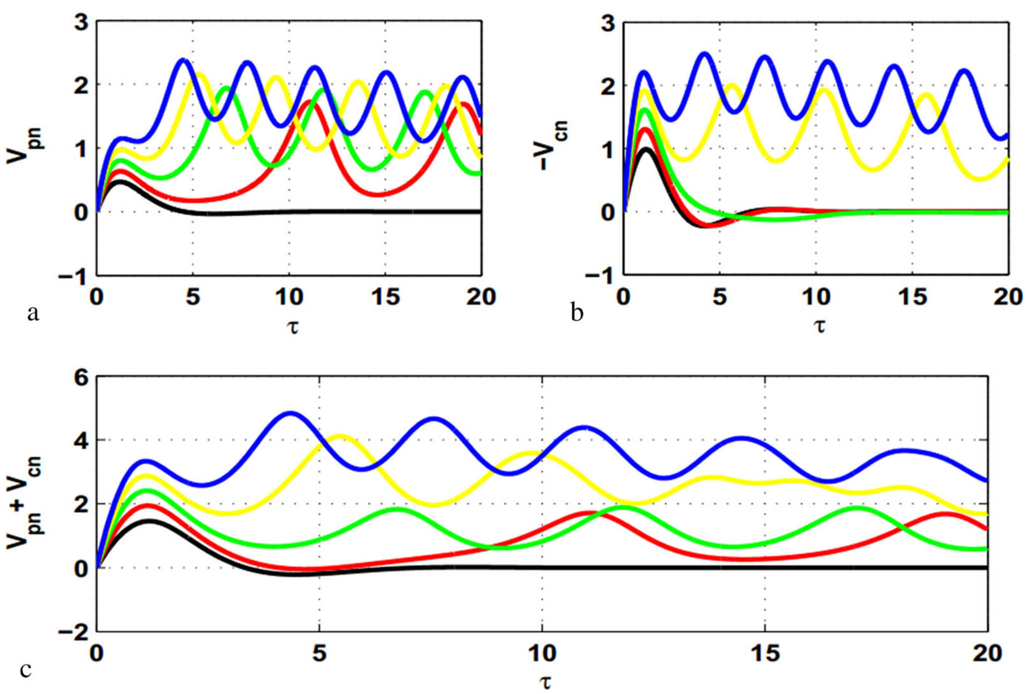

Figure 6. Time series of the AP for $i_{in} = 1.0$ and $i_b = 2.0$: (**a**) for the pulse junction V_{pn}, (**b**) for the control junction V_{cn} and (**c**) the net AP $V_{pn} + V_{cn}$. The black, red, green, yellow and blue curves are for the fifth, fourth, third, second and first JJ neuron circuit respectively.

incoming currents i_{in} and i_b in which system (4) is stable. Taking into consideration $i_{in} = 1.0$ and $i_b = 2.0$, which are values of the current pair out of the stability zone, the AP is observed to lose its shape and for five interconnected neurons, we have five AP in an unstable state as depicted in figure 6. These observations say a lot about the stability characterisation of system 4.

Figure 6 shows that the electromechanical system represented by system (4) fails to generate a membrane potential with sufficient intensity for actuation processes. This is the consequence of the excitation currents which are out of the stability domain of the system, hence the absence of a firing state in the system. For these values of currents in figure 6, the evolution of the

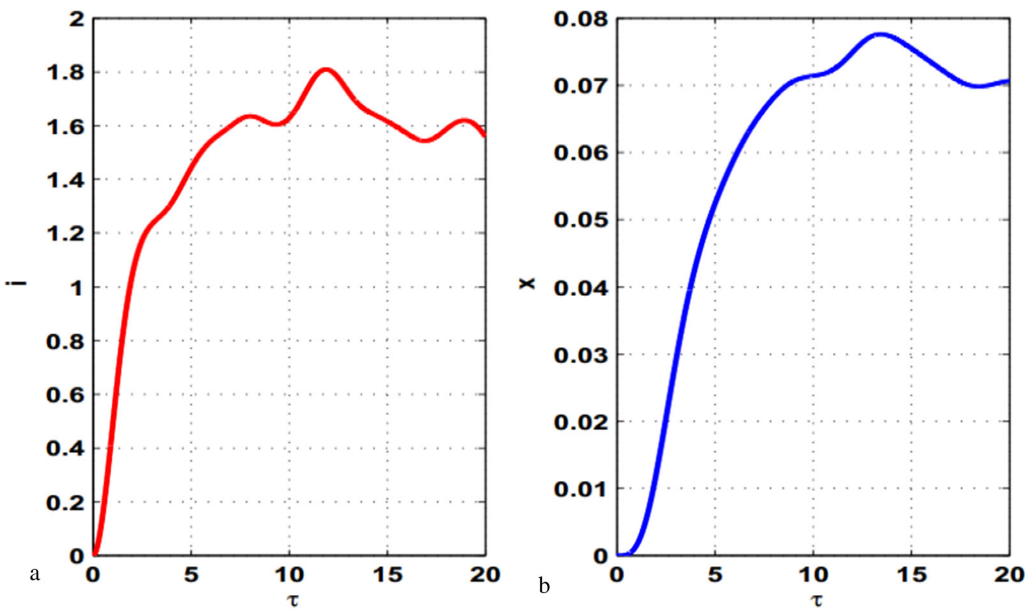

Figure 7. Time evolution of (**a**) the current i and (**b**) the instantaneous displacement x of the mobile beam for specific values of the currents $i_{in} = 1.0$ and $i_b = 2.0$.

current and the instantaneous displacement of the leg with time is presented in figure 7.

Figure 7 depicts that the current feeding the mechanical device and the displacement of the mechanical arm lose their transitory phase and tend to an infinite position. Furthermore, the investigation of the impact of the action of a magnetic field and the effect of mass on the evolution of the mechanical arm for various values of the magnetic field is presented in figure 8.

Figure 8 shows that the shift of the leg between the initial and final position decreases with an increase in the magnetic field. Thus, an increase in the electromagnetic field accelerates the motion of the legs. Also, the amplitude of displacement decreases with an increase in the mass and the displacement takes the form of a constant wave in some cases (black curve). It is interesting to highlight that varying the magnetic field and the effect of mass do not influence the AP when the system is in an excitable state.

3. Several lines of JJ neuron circuits coupled in actuating an array of mechanical legs

The circuit in figure 9 is made up of Mth preceding circuits of figure 1 coupled together. It is the device showing the propagation of electrical signals and the coordinate motion of M legs of the myriapods. Communication between the legs is blocked by coupling. There are many categories of coupling among which the unidirectional coupling between neurons was employed so that when one of the oscillators oscillates, the other remains at equilibrium, which does not move since in the JJ neuron circuit all the neurons are in-phase, thereby exchanging information from one neuron to another. These communications are ensured by axons modelled by resistance. From eq. (2), the incoming current has the form:

$$\begin{aligned} i_m \; &= \frac{\omega_\tau}{RI_{op}} \sum_{n=1}^{N} \left[\left(\frac{\phi_0}{2\pi} - l_p \lambda I_{op} \right) (\dot{\Phi}_{p(n,m-1)} \right. \\ &\quad + \dot{\Phi}_{p(n,m+1)} - 2\dot{\Phi}_{c(n,m)}) - l_p \lambda I_{op} (\dot{\Phi}_{c(n,m-1)} \\ &\quad \left. + \dot{\Phi}_{c(n,m+1)} - 2\dot{\Phi}_{c(n,m)}) \right] + i_b, \end{aligned} \tag{5}$$

with n representing the number of neurons and M the number of legs or mechanical devices (see eq. (5)). By employing Kirchhoff's and Newton's laws, the evolution of lattice depicted by the coupling device of figure 9 is modelled by a set of discrete nonlinear differential equations of system (6) for $2 \le m \le M - 1$ and $1 \le n \le N$: The coupling resistance is given by $R = NR_{\text{axon}}$, where R_{axon} is the resistance of one axon.

The nonlinear first-order differential equations of system (6) are obtained by employing Kirchhoff's and Newton's laws given as

$$\begin{aligned} \frac{\mathrm{d}V_{p(n,m)}}{\mathrm{d}\tau} &= -\Gamma V_{p(n,m)} - \sin(\Phi_{p(n,m)}) - \lambda(\Phi_{p(n,m)} \\ &\quad + \Phi_{c(n,m)}) + \left(\frac{1 - \Lambda_{pn}}{R} \right) \omega_\tau \end{aligned}$$

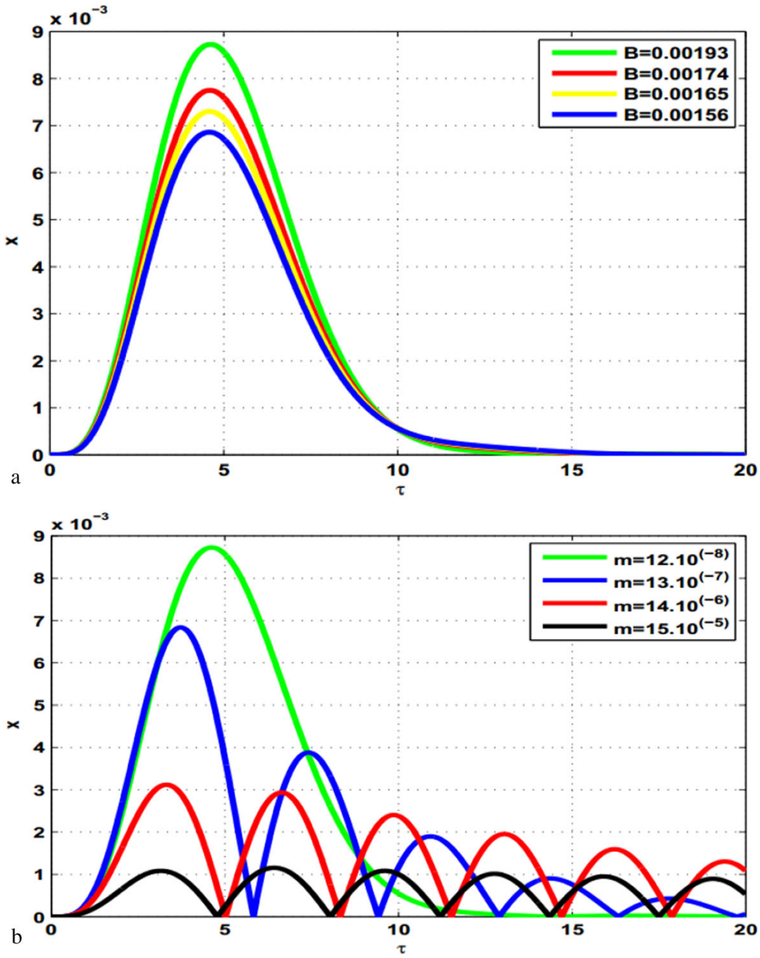

Figure 8. Time evolution in an excitable state of (**a**) the displacement of the mechanical arm with varying magnetic field for $B = 0.00193\,\mathrm{T}$ (green curve), $B = 0.00174\,\mathrm{T}$ (red curve), $B = 0.00165$ T (yellow curve) and $B = 0.00156\,\mathrm{T}$ (blue curve) and (**b**) the displacement of the mechanical arm with varying mass for $m = 12 \times 10^{-8}$ kg (green curve), $m = 13 \times 10^{-7}$ kg (blue curve), $m = 14 \times 10^{-6}$ kg (red curve) and $m = 15 \times 10^{-5}$ kg (black curve).

$$
\begin{aligned}
&+ \left(\frac{\phi_0}{2\pi I_{op}} - l_p\lambda\right)(V_{p(n,m-1)} + V_{p(n,m+1)} \\
&- 2V_{p(n,m)}) - \frac{(1-\Lambda_{pn})\omega_\tau l_p \lambda}{R}(V_{c(n,m-1)} \\
&+ V_{c(n,m+1)} - 2V_{c(n,m)}) + (1-\Lambda_{pn})i_b \\
&+ (\Lambda_{sn} + (1-\Lambda_{pn})(N-n))i_{in}, \qquad \text{(6a)}
\end{aligned}
$$

$$
\begin{aligned}
\frac{\mathrm{d}V_{c(n,m)}}{\mathrm{d}\tau} =& -\Gamma V_{c(n,m)} - \sin(\Phi_{c(n,m)}) - \lambda(\Phi_{p(n,m)} \\
&+ \Phi_{c(n,m)}) - \frac{\Lambda_{pn}\omega_\tau}{R} + \left(\frac{\phi_0}{2\pi I_{op}} - l_p\lambda\right) \\
&\times \left(V_{p(n,m-1)} + \times V_{p(n,m+1)} - 2V_{p(n,m)}\right) \\
&+ \frac{\Lambda_{pn}\omega_\tau l_p \lambda}{R}(V_{c(n,m-1)} + V_{c(n,m+1)} \\
&- 2V_{c(n,m)}) - \Lambda_{pn} i_b + (\Lambda_{sn} + (N-n))i_{in}, \qquad \text{(6b)}
\end{aligned}
$$

$$
\frac{\mathrm{d}\Phi_{p(n,m)}}{\mathrm{d}\tau} = V_{p(n,m)}, \tag{6c}
$$

$$
\frac{\mathrm{d}\Phi_{c(n,m)}}{\mathrm{d}\tau} = V_{c(n,m)}, \tag{6d}
$$

$$
\begin{aligned}
\frac{\mathrm{d}i_m}{\mathrm{d}\tau} =& \delta y_m - \sigma i_m + \rho \sum_{n=1}^{N} \left[\left(\frac{\phi_0}{2\pi} - \lambda L_p I_{op}\right)\right. \\
&\left. \times V_{p(n,m)} - \lambda L_p I_{op} V_{c(n,m)}\right],
\end{aligned} \tag{6e}
$$

$$
\frac{\mathrm{d}y_m}{\mathrm{d}\tau} = \mu i_m - \beta y_m - \gamma x_m, \tag{6f}
$$

$$
\frac{\mathrm{d}x_m}{\mathrm{d}\tau} = y_m, \tag{6g}
$$

with the same dimensionless parameters as in system (4). It is of great interest to highlight that the incoming current for the first and the M legs are respectively given

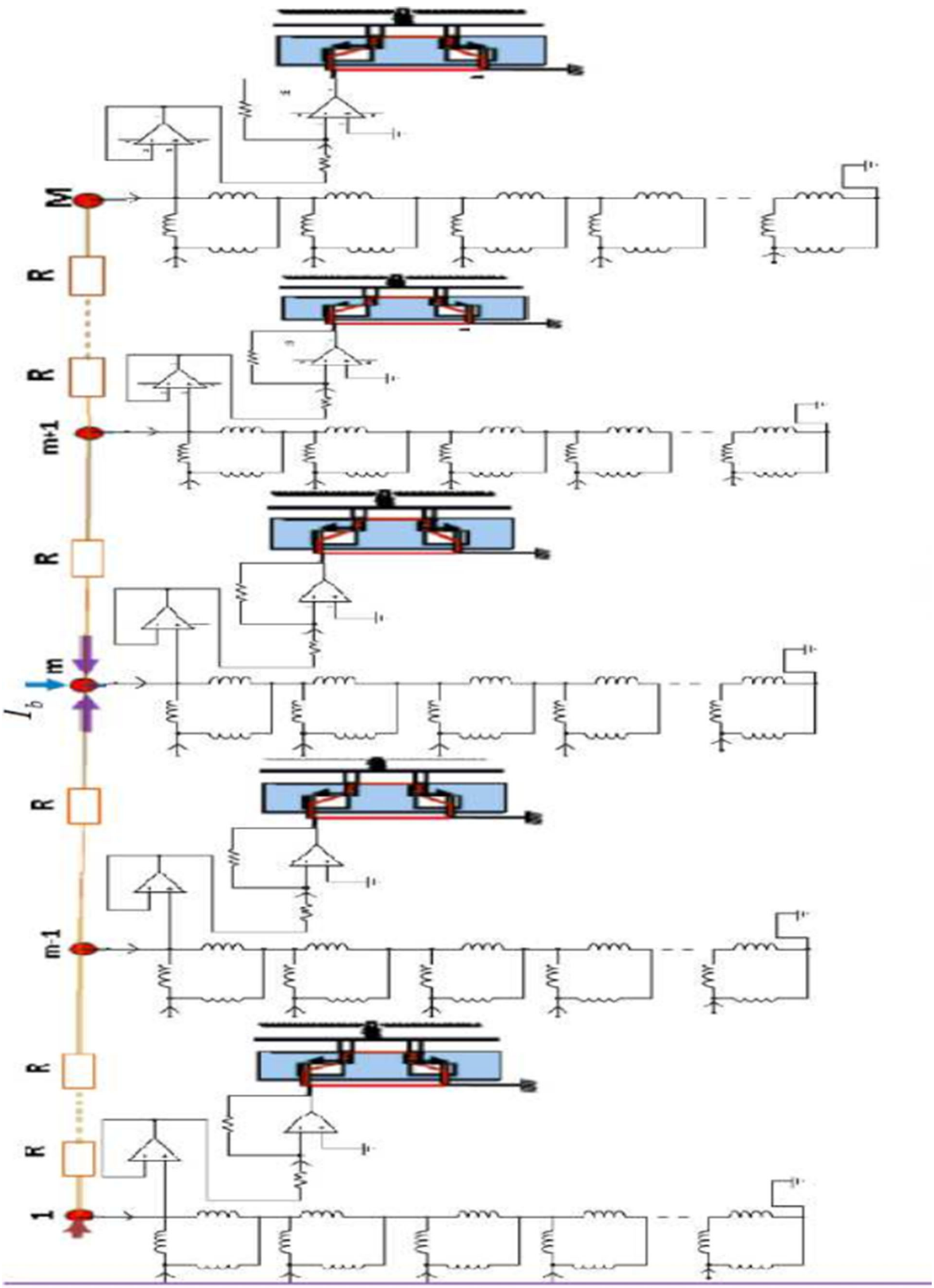

Figure 9. The coupled system of figure 1, mimicking the motion pattern of myriapods.

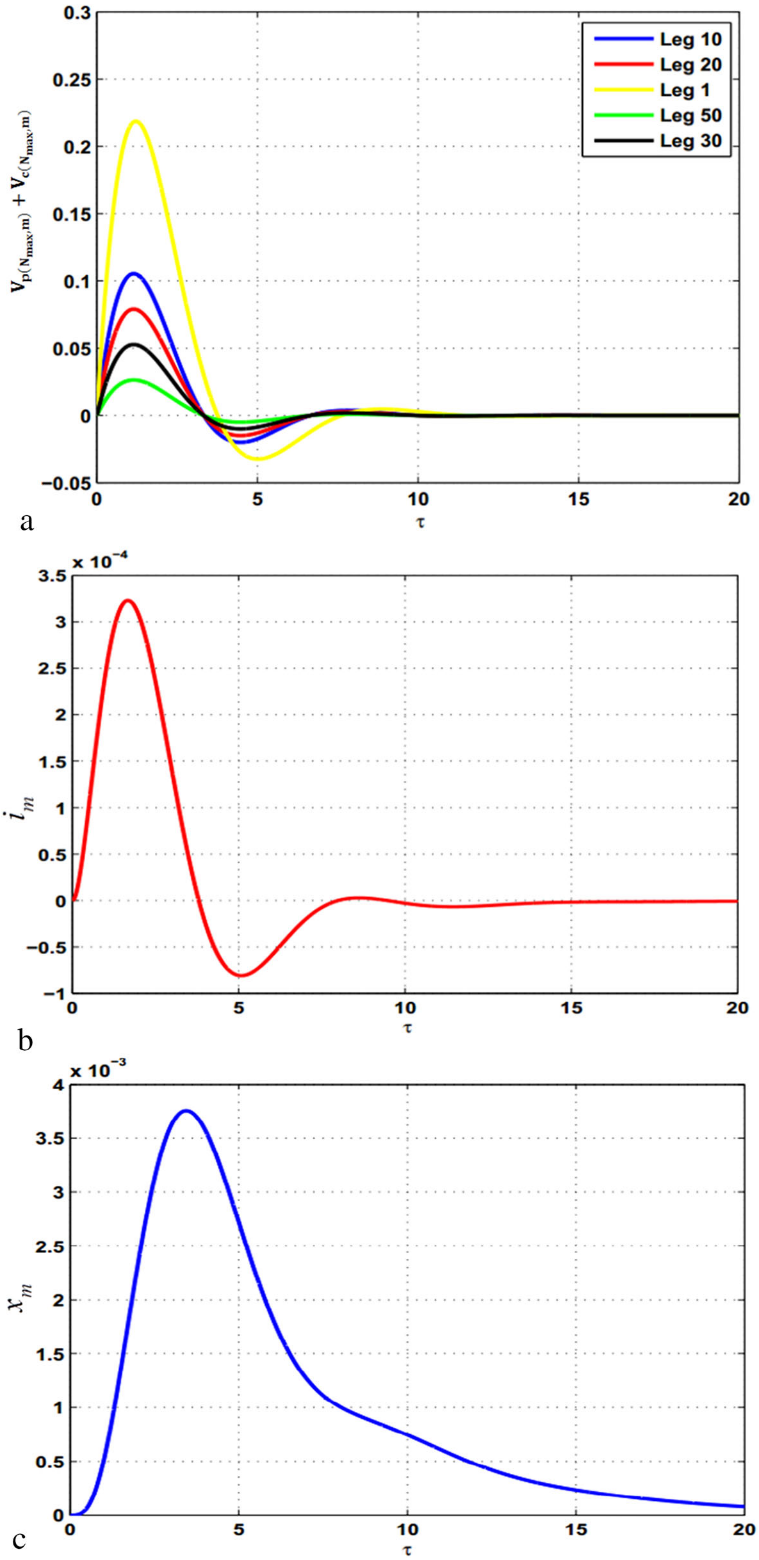

Figure 10. Time evolution for $m = 1,\ 10,\ 20,\ 30,\ 50$. (**a**) Net AP $V_{p(N_{\max},m)}V_{c(N_{\max},m)}$ for $N_{\max} = 200$, (**b**) the current i_m and (**c**) two-dimensional representation of the displacement x_m.

by eqs (7a) and (7b) as

$$i_1 = \frac{\omega_\tau}{RI_{op}}\left(\left(\frac{\phi_0}{2\pi} - l_p\lambda I_{op}\right)(\dot{\Phi}_{p(n,2)} - \dot{\Phi}_{p(n,1)}) - l_p\lambda I_{op}(\dot{\Phi}_{c(n,2)} - \dot{\Phi}_{c(n,1)})\right) + i_b, \tag{7a}$$

$$i_M = \frac{\omega_\tau}{RI_{op}}\left(\left(\frac{\phi_0}{2\pi} - l_p\lambda I_{op}\right)(\dot{\Phi}_{p(n,M-1)} - \dot{\Phi}_{p(n,M)}) - l_p\lambda I_{op}(\dot{\Phi}_{c(n,M-1)} - \dot{\Phi}_{c(n,M)})\right) + i_b. \tag{7b}$$

The starting condition for system (6) is given by

$$V_{c(n,m)} = V_{p(n,m)} = i_m = x_m = y_m = \Phi_{c(n,m)} = 0, \tag{8a}$$

$$\Phi_{p(n,m)} = \arcsin(i_{b(m)} - \Lambda_p(N_{max} - 1)i_{in}). \tag{8b}$$

The AP, the current powering the mechanical device and the instantaneous displacement of the legs are presented in figure 10.

The observation of the AP in figure 10a depicts that the curves are superposed and their amplitudes decrease as the number of legs increases. There is no propagation of the signal of AP for simulating the multilegged locomotion. This result is not normal because one property of the AP is the 'All or nothing' law [69] and propagation without attenuation of the signals. But in this case, the signal does not propagate in the network. The same current is observed for all the legs plotted as depicted in figure 10b and the effect of such current feeding the mechanical arms resulted in the superposition of all the legs as shown in figure 10b. Finally, with this model of the array of JJ neuron circuits coupled to the mechanical device, there is no propagation of the signals. This is because the stimulation is not well known and the 'All or nothing' law is not respected. This permits the conclusion that this JJ neuron model has the shape of the action potential but does not have all the properties of the action potential like stimulation and propagation of the signal. It is not a good neuron because it does not propagate its signal in the neuronal structures. A good artificial neuron has a defined stimulation and can propagate its signal in a network [70–72], which is capable of simulating the motion of myriapods.

4. Conclusion

This paper studied the effect of an artificial neuron model by coupling an array of coupled JJ neuron circuits of a mechanical arm to which is attached a leg. The rate equations for the proposed electromechanical system were established. Numerical simulations of the electromechanical system resulted in well-defined action potential and subsequently the actuation of the leg attached to the mechanical arm in an excitable state. Furthermore, the impact of the action of the electromagnetic signal and the effect of mass showed that an increase in the magnetic field strength accelerates the motion of the legs and the amplitude of displacement decreases with an increase in the mass and the displacement takes the form of a constant wave for some particular masses as shown by the numerical simulations. This model failed to propagate the signal in an array of legs. There is no propagation, because, each neuron produces its signal at the same time and this problem comes because the stimulation is not well defined by this model of the JJ neuron circuit, despite the advantages of the JJ neuron circuits. The outcomes of the proposed electromechanical system led to the suggestion for further studies in which it will be interesting to consider a new JJ neuron circuit with a well-defined stimulation current to overcome the challenges in the later model.

Acknowledgement

This work is partially funded by the Centre for Nonlinear Systems, Chennai Institute of Technology, India via funding number CIT/CNS/2023/Rp-007.

References

[1] M Canturk and I N Askerzade, *J. Supercond. Nov. Magn.* **26**, 839 (2013)
[2] I K Ngongiah, B Ramakrishnan, Z T Njitacke, G F Kuiate and S T Kingni, *Phys. A Stat. Mech. Appl.* **603**, 127757 (2022)
[3] J Ramadoss, I K Ngongiah, A C Chamgoué, J R Mboupda Pone, K Rajagopal and S T Kingni, *Phys. Scr.* **96**, 1252321 (2021)
[4] S T Kingni, G F Kuiate, R Kengne, R Tchitnga and P Woafo, *Complexity* **2017**, 1 (2017)
[5] E M Shahverdiev, L H Hashimova, P A Bayramov and R A Nuriev, *J. Supercond. Nov. Magn.* **27**, 2225 (2014)
[6] S Sancho and A Suarez, *IEEE Trans. Circuits Syst. I: Regul. Pap.* **61**, 512 (2014)
[7] S K Dana, D C Sengupta and K D Edoh, *IEEE Trans. Circuits Syst. I: Fundam. Theory Appl.* **48**, 990 (2001)
[8] G Filatrella, N F Pedersen, C J Lobb and P Barbara, *Eur. Phys. J. B* **34**, 3 (2003)
[9] I Borodianskyi, *Superradiant THz wave emission from arrays of Josephson junctions*, Doctoral dissertation

(Department of Physics, Stockholm University, 2020) pp. 1–67
[10] A Uchida, H Iida, N Maki, M Osawa and S Yoshimori, *IEEE Trans. Appl. Supercond.* **14**, 2064 (2004)
[11] R Kleiner, P Müller, H Kohlstedt, N F Pedersen and S Sakai, *Phys. Rev. B* **50**, 3942 (1994)
[12] D Domínguez and H A Cerdeira, *Phys. Rev. B* **52**, 513 (1995)
[13] N Vogt *et al*, *Phys. Rev. B* **92**, 045435 (2015)D
[14] D Crété *et al*, *Micromachines* **12**, 1588 (2021)
[15] R Glowinski, J López, H Juárez and Y Braiman, *J. Comput. Phys.* **403**, 109023 (2020)
[16] J C LeFebvre, E Cho, H Li, H Cai and S A Cybart, *J. Appl. Phys.* **131**, 163902 (2022)
[17] N M Kouami, B Nana and P Woafo, *Phys. C Supercond. Appl.* **574**, 1 (2020)
[18] R Harris *et al*, *Phys. Rev. B* **80**, 052506 (2009)
[19] G M Ngueuteu, R Yamapi and P Woafo, *J. Sound Vib.* **318**, 1119 (2008)
[20] H H Lund, *Human aspects of IT for the aged population. Design for Everyday Life* (Springer-Verlag, 2015) Vol. 9194, p. 500
[21] H H Lund and J D Jessen, *GAMES Heal. Res. Dev. Clin. Appl.* **3**, 277 (2014)
[22] M Sood and S W Leichtle, *Essentials of robotic surgery* (Spry Publishing, 2013)
[23] T D Coates, *Neural interfacing, forging the human-machine connection* (Morgan and Clayton Publishers, 2008)
[24] I R Nourbakhsh, *Robot futures* (The MIT Press, Massachusetts, 2013)
[25] J L Pons, *Wearable robots: Biomechatronic exoskeletons* (John Wiley and Sons Ltd., 2008)
[26] S Kajita, H Hirukawa, K Harada and K Yokoi, *Introduction to humanoid robotics* (Springer, 2014)
[27] S Y Nof, *Springer handbook of automation* (Springer-Verlag, 2008)
[28] R Siegwart, I R Nourbakhsh and D Scaramuzza, *Introduction to autonomous mobile robots* (The MIT Press, Massachusetts, 2004)
[29] J Gerhart, *Home automation and wiring* (McGraw Hill Professional, 1999)
[30] P J Springer, *Military robots and drones: A reference handbook* (ABC-CLIO, 2013)
[31] R D Launius and H E McCurdy, *Robots in space: Technology, evolution and interplanetary travel* (The Johns Hopkins University Press, Baltimore, 2008)
[32] R Malone, *Ultimate robot* (DK Pub., 2004)
[33] L Pagliarini and H H Lund, *AROB, 13th International Symposium on Artificial Life and Robotics* (Oita, Japan, 31 January–2 February 2008)
[34] R Hanson, *The age of Em: Work, love and life when robots rule the Earth* (Oxford University Press, 2016)
[35] S Kernbach, *Handbook of collective robotics: Fundamentals and challenges* (Pan Stanford Publishing, 2013)
[36] K Stay, D Brandt and D J Christensen, *Self-reconfigurable robots. An Introduction* (MIT Press, 2010)
[37] K Meruva and Z Bi, *Proceedings of the IEEE International Conference on Information and Automation* (Ningbo, China, August 2016) pp. 299–304
[38] L Nocks, *The robot: The life story of a technology* (Greenwood Publishing Group, 2007)
[39] K Akimoto, S Watanabe and M Yano, *Pro. Intl. Symposium on Artificial Life and Robotics* (1999) Vol. 3, pp. 102–105
[40] R R Brooks, *IEEE J. Robot. Autom.* **RA-2**, 14 (1986)
[41] R A Brooks, *Neural Comput.* **1**, 253 (1989)
[42] K Tsujita, A Onat, K Tsuchiya and Y Kawano, *Proc. 5th Intl. Symposium on Artificial Life and Robotics* (2000) pp. 703–710
[43] K Tsujita, K Tsuchiya, A Onat, S Aoi and M Kawakami, *Proc. of the Sixth International Symposium of Artificial Life and Robotics* (2001) Vol. 2, pp. 421–426
[44] J J Collins and S A Richmond, *Biol. Cybern.* **71**, 375 (1994)
[45] J J Collins and I Stewart, *J. Nonlinear Sci.* **3**, 349 (1993)
[46] C Gehring, S Coros, M Hutter, M Bloesch, M A Hoepflinger and R Siegwart, *IEEE International Conference on Robotics and Automation* (2013) pp. 3287–3292
[47] Q Cao, A T Van Rijn and I Poulakakis, *IEEE/RSJ International Conference on Intelligent Robots and Systems (IROS)* (2015) pp. 5136–5141
[48] D Owaki and A Ishiguro, *Sci. Rep.* **7**, 1 (2017)
[49] Y Yang, T Zhang, E Coumans, J Tan and B Boots, *Conference on Robot Learning* (2022) pp. 773–783
[50] V Tsounis, M Alge, J Lee, F Farshidian and M Hutter, *IEEE Robot. Autom. Lett.* **5**, 3699 (2020)
[51] A H Cohen, P J Holmes and R H Rand, *J. Math. Biol.* **13**, 345 (1982)
[52] R H Rand, A H Cohen and P J Holmes, *Neural control of rhythmic movements in vertebrates* edited by A H Cohen, S Rossignol and S Grillner (Wiley, New York, 1988) pp. 333–367
[53] K Qiu, H Zhang, Y Lv, Y Wang, C Zhou and R Xiong, *IEEE International Conference on Real-time Computing and Robotics (RCAR)* (2021) pp. 468–473
[54] T G Deliagina, P E Musienko and P V Zelenin, *Curr. Opin. Physiol.* **8**, 7 (2019)
[55] A Athota, B Caccam, R Kochis, A Ray, G Cauwenberghs and F D Broccard, *43rd Annual International Conference of the IEEE Engineering in Medicine and Biology Society (EMBC)* (2021) pp. 6703–6706
[56] J Knüsel, A Crespi, J M Cabelguen, A J Ijspeert and D Ryczko, *Front. Neurorobot.* **14**, 604426 (2020)
[57] N Kopell and G B Ermentrout, *Commun. Pure Appl. Math.* **39**, 623 (1986)
[58] N Kopell and G B Ermentrout, *Math. Biosci.* **89**, 14 (1988)
[59] N Kopell and G B Ermentrout, *SIAM J. Appl. Math.* **50**, 1014 (1990)
[60] R Yamapi, J C Ourou and P Woafo, *Int. J. Bifurc. Chaos* **14**, 171 (2004)

[61] P Crotty, D Schult and K Segall, *Phys. Rev. E* **82**, 0119141 (2010)
[62] A H Lewis and I M Raman, *J. Physiol.* **592**, 4825 (2014)
[63] J S Yeomans, *Physiol. Behav.* **22**, 911 (1979)
[64] M Milosavljevic and M Cerf, *Int. J. Advert.* **27**, 381 (2008)
[65] I Blundell *et al*, *Front. Neuroinform.* **12**, 1 (2018)
[66] R A McDougal *et al*, *J. Comput. Neurosci.* **42**, 1 (2017)
[67] D T Ngatcha, A A Oumate, A S K Tsafack and S T Kingni, *Chaos Theory Appl.* **3**, 55 (2021)
[68] B Ramakrishnan, L M A Tabejieu, I K Ngongiah, S T Kingni, R T Siewe and K Rajagopal, *J. Supercond. Nov. Magn.* **34**, 2761 (2021)
[69] H Dziubinska, A Paszewski, K Trebacz and T Zawadzki, *Physiol. Plant.* **57**, 279 (1983)
[70] F Patolsky *et al*, *Science* **313**, 1100 (2006)
[71] T P Vogels and L F Abbott, *J. Neurosci.* **25**, 10786 (2005)
[72] J C Whittington and R Bogacz, *Trends Cogn. Sci.* **23**, 235 (2019)